In Situ Measurements of Interface States at Silicon Surfaces in Fluoride Solutions

Gerko Oskam, Peter M. Hoffmann, and Peter C. Searson

Department of Materials Science and Engineering, The Johns Hopkins University, Baltimore, Maryland 21218

(Received 22 June 1995)

The energetics and kinetics of processes involving interface states at silicon (111) surfaces in aqueous fluoride solutions were determined using *in situ* impedance spectroscopy. In the dark, we observe electrically active surface states with densities in the range 2×10^{10} to 1×10^{12} cm^{-2} dependent on the surface chemistry. The surface states are physically the same, independent of *p*H, with a capture cross section of 1×10^{-16} cm^2. Measurements under illumination show that recombination occurs at different interface states than those observed in the dark.

PACS numbers: 73.40.Mr, 72.20.Jv, 73.20.At, 82.45.+z

In recent years there has been renewed interest in the surface properties of silicon. In particular, the decreasing feature sizes in electronic devices have highlighted the importance of wafer cleaning and surface preparation. Chemical methods are routinely used in the cleaning and passivation of silicon surfaces, and many of these processes involve immersion in HF solutions [1,2]. It was first recognized, more than 10 years ago, that immersion of silicon in HF results in a hydrogen passivated surface [3] with a very low surface recombination velocity [4]. More recently it has been shown that the morphology of hydrogen passivated silicon surfaces is dependent on crystal orientation and *p*H [5,6]. At low *p*H, the Si(111) surface is essentially unreactive, whereas at higher *p*H the etch rate for weakly coordinated Si-H_2 and Si-H_3 surface sites becomes significant resulting in the formation of large domains of ideally terminated Si(111): H(1×1) terraces [7–10]. In order to fully exploit the chemical and structural modification of silicon surfaces for device applications, it is desirable to have *in situ* techniques to relate the surface chemistry to the electrical properties. The purpose of this Letter is twofold. First, we show that the energetics and kinetics of processes involving interface states at semiconductor surfaces can be determined in an electrolyte solution. Second, we demonstrate that two types of electrically active interface states are present at silicon surfaces in aqueous solutions whose properties depend strongly on the *p*H of the solution.

All measurements were performed on *n*-Si(111) ($N_D = 3 \times 10^{13}$ cm^{-3}). The wafers were RCA cleaned [1] and immersed in 49 wt.% HF for 5 min prior to each experiment. All measurements in the dark were performed in 1*M* NH_4F, adjusted to the desired *p*H by addition of HF or NH_4OH. For experiments under illumination, $K_4Fe(CN)_6$ and KCl were added to the solution in order to stabilize the surface and minimize photocorrosion [11].

Surface states at an *n*-type semiconductor in the dark interact with the conduction band (CB), as shown in Fig. 1(a). If the states are energetically close to the CB and interaction with the solution can be neglected, the occupancy is determined by the position of the Fermi level at the surface. The capture of electrons from the conduction band and thermal detrapping from the surface states can be described by the following equations:

$$SS^0 + e^-(CB) \xrightarrow{k_1} SS^-, \tag{1a}$$

$$SS^- \xrightarrow{k_2} SS^0 + e^-(CB). \tag{1b}$$

The impedance due to filling and emptying of the surface states can be calculated by considering the harmonic response to a sinusoidal voltage modulation. For a small modulation amplitude, the modulated density of occupied surface states $\tilde{s}^-$ is given by

$$\frac{d\tilde{s}^-}{dt} = i\omega\tilde{s}^- = k_1 n_s \tilde{s}^0 + k_1 s^0 \tilde{n}_s - k_2 \tilde{s}^-, \tag{2}$$

where $\tilde{s}^0$ is the modulated density of empty states ($\tilde{s}^0 = -\tilde{s}^-$), $\tilde{n}_s$ is the modulated surface electron concentration, $i = \sqrt{-1}$, and ω is the angular frequency. The surface electron concentration is described by a Boltzmann distribution and for a small modulation amplitude we obtain

$$\tilde{n}_s = -n_s \frac{e}{kT} \tilde{U}, \tag{3}$$

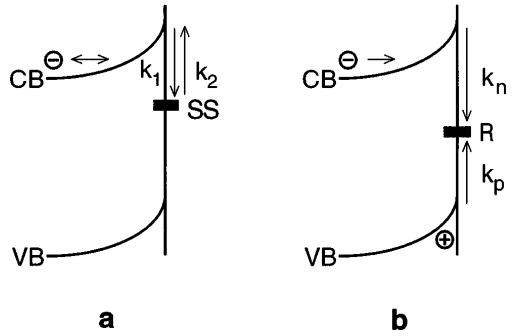

FIG. 1. Energy band diagrams illustrating the processes at occurring at interface states for an *n*-type semiconductor. (a) Electrons in the conduction band (CB) can be trapped and detrapped from surface states with respective rate constants k_1 and k_2. (b) Under illumination, free holes and electrons can be trapped on recombination centers with rate constants denoted by k_p and k_n.

where $\tilde{U}$ is the potential modulation. The modulated electron flux $\tilde{j}$ resulting from the modulation of the applied potential is obtained from (2) and (3),

$$\tilde{j} = \frac{d\tilde{s}^-}{dt} = -\frac{e}{kT} k_1 n_s s^0 \frac{i\omega}{i\omega + k_2 + k_1 n_s} \tilde{U}. \quad (4)$$

The impedance due to relaxation of the surface states is given by

$$Z_{ss} = -\frac{\tilde{U}}{e\tilde{j}} = \frac{kT}{e^2} (k_1 n_s s^0)^{-1} \left(1 + \frac{k_1 n_s + k_2}{i\omega}\right). \quad (5)$$

Equation (5) shows that the surface state impedance Z_{ss} is equivalent to a resistance in series with a capacitance. Since Z_{ss} is in parallel with the space charge layer capacitance C_{sc}, it is convenient to consider an equivalent parallel combination of C_{sc} with a frequency dependent surface state capacitance, $C_p(\omega)$ [12],

$$C_p(\omega) = \frac{e^2}{kT} \left(\frac{k_2 k_1 n_s}{\omega^2 + (k_1 n_s + k_2)^2}\right) N_{ss}, \quad (6)$$

where N_{ss} is the density of surface states. $C_p(\omega)$ may be evaluated experimentally by subtracting space charge capacitance from the measured parallel capacitance. The corresponding parallel conductance obtained from this model is equivalent to the result obtained by Nicollean and Goetzberger [13] who used a thermodynamic model to determine the density of states at Si/SiO_2 interfaces in metal-oxide-semiconductor devices.

The density of surface states and the relevant rate constants can be determined experimentally by considering the frequency dependence of Eq. (6). At low frequencies, where $\omega^2 \ll (k_1 n_s + k_2)^2$, C_p exhibits a maximum as a function of potential at $k_1 n_s = k_2$ corresponding to an occupancy of 0.5. The capacitance at the maximum, $C_p(\max)$, is related to the density of surface states by

$$C_p(\max) = \frac{1}{4} \frac{e^2}{kT} N_{ss}. \quad (7)$$

Figure 2 shows the measured parallel capacitance, after subtraction of the space charge component [14], vs applied potential for an n-Si(111) surface in NH_4F solution at pH4. The frequency dependence of the surface state capacitance, in the inset in Fig. 2, shows a plateau at frequencies below 1 kHz. At frequencies above 10 kHz where $\omega^2 \gg (k_1 n_s + k_2)^2$, the slope approaches -2, in agreement with Eq. (6), indicating a monoenergetic surface state. The full width at half maximum of the capacitance peak in Fig. 2 is about 0.1 V, in good agreement with the predicted value of $3.52kT/e$ for a monoenergetic surface state [15]. From the position of the peak maximum, the surface state energy was determined to be 0.38 eV below the conduction band edge.

The rate constants k_1 and k_2 can be obtained by recognizing that at the roll-off frequency $\omega^2 = (k_1 n_s + k_2)^2$ and $k_1 n_s = k_2$ at the potential of the capacitance maximum. From Fig. 2, the rate constants for filling (k_1) and emptying (k_2), the surface states were determined to be 2×10^{-9} cm^3 s^{-1} and 2×10^4 s^{-1}, respectively. From k_2 the capture cross section of the surface states was found to be 1×10^{-16} cm^2 [16], corresponding to approximately a single lattice site. Values for N_{ss}, k_1, and k_2 obtained from analysis of the parallel conductance were in agreement with those obtained from the parallel capacitance, confirming that both the real and imaginary components are consistent with the simple model shown in Fig. 1(a).

Figure 3 shows the surface state density, calculated from Eq. (7), plotted as a function of pH. At low pH the hydrogen passivated surface is stable, and the surface state density is about 2×10^{10} cm^{-2}, in agreement with recent *in situ* microwave measurements [17]. At higher pH the surface state density increases to about 1×10^{12} cm^{-2}, characteristic of a chemically oxidized surface. Both the hydrogen passivated and oxide passivated surfaces were stable during extended immersion with no change in the density of surface states. The surface state energy was essentially independent of pH, suggesting that the surface states are physically the same for both hydrogen passivated and oxide passivated surfaces.

The sharp increase in surface state density around pH7 is related to the formation of an oxide layer. At positive potentials and at high pH, oxide formation can no longer be suppressed due to the low concentration of molecular HF [18]. In contrast, the hydrogen passivated surface is reported to be stable up to very high pH at the open circuit potential [2]. These results demonstrate a limited domain of thermodynamic stability for the hydrogen passivated surface as a function of pH and applied bias.

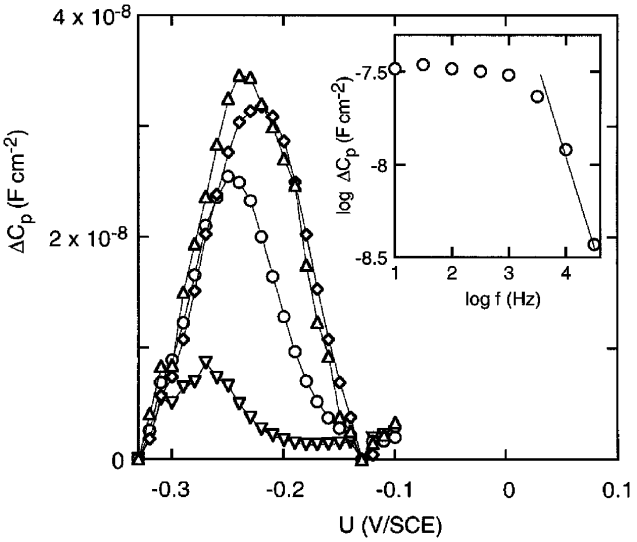

FIG. 2. The parallel surface state capacitance vs applied potential in 1M NH_4F at pH4: 31.6 Hz (Δ), 316 Hz (◇), 3.16 kHz (○), and 31.6 kHz (▽). The inset shows the frequency dependence of C_p at -0.24 V (SCE). The solid line corresponds to the predicted slope of -2.

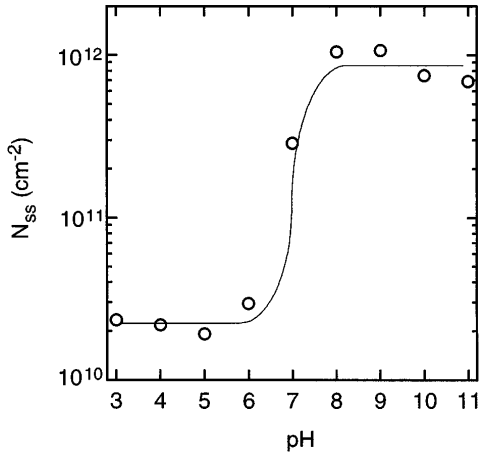

FIG. 3. Surface state density, obtained using Eq. (7), vs pH for n-Si(111) surfaces in 1M NH_4F solutions.

Recombination processes were analyzed as a function of both light intensity and band bending using photoelectrochemical impedance spectroscopy. Under illumination at pH9, the measured parallel capacitance exhibits two maxima, as shown in Fig. 4. The peak at -0.5 V corresponds to the surface states observed in the dark and obeys the frequency dependence described in Eq. (6). The second peak at 0.2 V is observed only under illumination, and the peak position, peak width, and peak height are dependent on frequency and light intensity. These features are characteristic of a surface recombination process [19], as shown schematically in Fig. 1(b). At high frequencies and assuming complete recombination ($j_{\mathrm{rec}} = j_h$), the recombination capacitance [20], calculated using the same approach as for the surface states, shows a maximum as a function of potential at $\omega = k_n n_s$ according to

$$C_{\mathrm{rec}}(\max) = \frac{e}{2kT}\,\frac{i_{\mathrm{ph}}}{\omega}\,, \tag{8}$$

where j_h is the minority carrier flux and $i_{\mathrm{ph}} = e j_h$, the photocurrent plateau at large band bending. At low frequency, $C_{\mathrm{rec}}(\max)$ becomes independent of frequency, and the limiting value for $\omega \to 0$ is given by

$$C_{\mathrm{rec}}(\max)_{\omega\to 0} = \frac{4}{27}\,\frac{e^2}{kT}\,N_{\mathrm{rec}}\,. \tag{9}$$

At high frequencies the experimental data follow Eq. (8) with slopes close to the predicted value of 20 V^{-1}, as shown in the inset in Fig. 5. At low frequencies, a frequency independent maximum is observed below about 5 Hz, and the density of recombination centers N_{rec} can be determined from Eq. (8). To our knowledge, this frequency independent maximum has not been reported previously.

Figure 5 shows the density of recombination centers vs the plateau photocurrent at pH9. For low photocurrents, N_{rec} increases from about 5×10^{11} cm^{-2} to about 4×10^{12} cm^{-2}. The plateau value at higher light intensities, corresponding to a capacitance of 4 μF cm^{-2}, is due to the limit where $C_{\mathrm{rec}}(\max) > C_H$, the Helmholtz capacitance, so that $C_{\mathrm{rec}}(\max)$ can no longer be determined. These results show that the density of recombination centers increases with increasing light intensity, indicating that recombination takes place at oxidation intermediates. Under illumination the hydrogen terminated surface is unstable, and the surface is passivated by an oxide

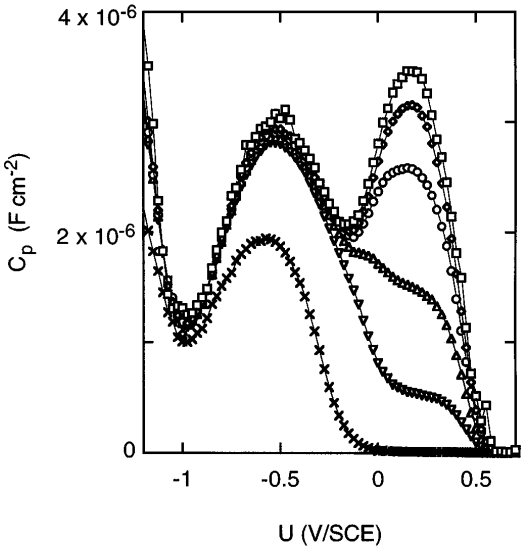

FIG. 4. The measured parallel capacitance vs applied potential for n-Si(111) in 1M NH_4F + 0.1M $K_4Fe(CN)_6$ + 0.5M KCl at pH9 under illumination: 2.15 Hz (□), 10 Hz (◇), 21.5 Hz (○), 46.4 Hz (Δ), 100 Hz (∇), and 1000 Hz (×). The plateau photocurrent i_{ph} was 35 μA cm^{-2}.

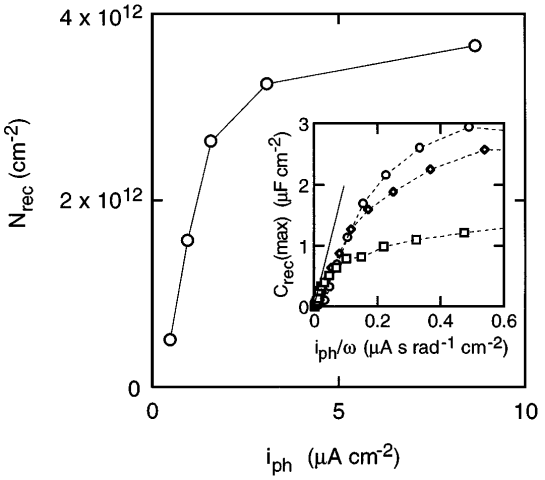

FIG. 5. The density of recombination centers N_{rec} vs the plateau photocurrent density i_{ph} [see Eq. (9)]. The inset shows $C_{\mathrm{rec}}(\max)$ vs i_{ph}/ω for $i_{\mathrm{ph}} = 0.94\mu$A cm^{-2} (□), $i_{\mathrm{ph}} =$ 1.6 μA cm^{-2} (◇), and $i_{\mathrm{ph}} = 3.1$ μA cm^{-2} (○). The solid line shows a slope of 20 V^{-1}.

layer, suggesting that the oxidation intermediates are related to incompletely oxidized silicon sites at the Si/SiO_2 interface.

The observation of a second capacitance peak under illumination suggests that the recombination centers are physically different from the surface states measured in the dark. This was confirmed by calculating the impedance for recombination occurring at the surface states; in this case only one capacitance peak is obtained, and the magnitude of the capacitance maximum is attenuated [21]. We can therefore exclude the possibility that the same states are responsible for the two peaks observed in Fig. 4.

The rate constant for recombination can be obtained from the capacitance peak shown in Fig. 4. From Mott-Schottky measurements, the band bending at the capacitance maximum (21.5 Hz) was determined to be about 0.12 eV. Making the usual assumption that $k_n n_s > k_p p_s$ (p_s is the surface concentration of free holes) and calculating n_s from the band bending and donor density, the rate constant for recombination k_n is found to be about 3×10^{-10} $cm^3\,s^{-1}$. This value was confirmed by intensity modulated photocurrent spectroscopy [21]. We note that k_n is about four orders of magnitude smaller than the value reported for n-GaAs, illustrating that recombination is much slower at silicon surfaces [22].

The authors gratefully acknowledge support from the National Science Foundation under Grant No. DMR-9202645.

[1] W. Kern and D. A. Puotinen, RCA Review **31**, 187 (1970).
[2] G. S. Higashi and Y. J. Chabal, in *Handbook of Semiconductor Wafer Cleaning Technology*, edited by W. Kern (Noyes, Park Ridge, 1994), p. 433.
[3] H. Ubara, T. Imura, and A. Hiraki, Solid State Commun. **50**, 673 (1984).
[4] E. Yablonovitch, D. L. Allara, C. C. Chang, T. Gmitter, and T. B. Bright, Phys. Rev. Lett. **57**, 249 (1986).
[5] P. Jakob, Y. J. Chabal, K. Raghavachari, R. S. Becker, and A. J. Becker, Surf. Sci. **275**, 407 (1992).
[6] H. E. Hessel, A. Feltz, M. Reiter, U. Memmert, and R. J. Behm, Chem. Phys. Lett. **186**, 275 (1991).
[7] G. S. Higashi, R. S. Becker, Y.hJ. Chabal, and A. J. Becker, Phys. Rev. Lett. **58**, 1656 (1991).
[8] R. S. Becker, G. S. Higashi, Y. J. Chabal, and A. J. Becker, Phys. Rev. Lett. **65**, 1917 (1990).
[9] G. W. Trucks, K. Raghavachari, G. S. Higashi, and Y. J. Chabal, Phys. Rev. Lett. **65**, 504 (1990).
[10] Y. Morita, K. Miki, and H. Tokumoto, Appl. Phys. Lett. **59**, 1347 (1991).
[11] B. H. Loo, K. W. Frese, and S. R. Morrison, Surf. Sci. **109**, 75 (1981).
[12] $C_p(\omega) = \omega\,\mathrm{Im}(Z)/(1 + D^2)$ where $D = [\{\mathrm{Re}(Z) - R_\Omega\}/ - \mathrm{Im}(Z)]$, where R_Ω is the high frequency series resistance and Z is the measured impedance.
[13] E. H. Nicollean and A. Goetzberger, Bell Syst. Tech. J. **46**, 1055 (1967).
[14] At positive potentials ($E_F < E_{ss}$) the impedance spectra exhibited a single time constant (due to the impedance of the space charge layer) over the measured frequency range (1 Hz–100 kHz); the corresponding Mott-Schottky plots were linear and virtually independent of frequency in this potential range. At potentials close to the flatband potential, a capacitance peak due to the surface states was superimposed on the space charge layer capacitance. The capacitance due to the surface states ΔC_p was obtained by subtraction of the underlying space charge capacitance ($\Delta C_p = C_p - C_{sc}$). In all cases, C_{sc} was at least one order of magnitude smaller than the low frequency capacitance maximum.
[15] The full width at half maximum was obtained from Eq. (6) by determining the change in n_s to give $C_p = C_p\,(\mathrm{max})/2$ in the low frequency limit where $\omega^2 = (k_1 n_s + k_2)^2$. The FWHM, in terms of the applied bias is $3.52kT/e$ (90 mV at room temperature).
[16] The capture cross section σ was calculated from the relation $k_2 = \nu_{th}\sigma N_c \exp[-(E_t - E_c)kT]$ taking the thermal velocity of electrons, $\nu_{th} = 10^7$ $cm\,s^{-1}$, the effective density of states in the CB, $N_c = 2.8 \times 10^{19}$ cm^{-3}, and the trap energy $(E_t - E_c) = 0.38$ eV.
[17] G. Schlichthörl and L. M. Peter, J. Electrochem. Soc. **141**, L171 (1994).
[18] J. S. Judge, J. Electrochem. Soc. **118**, 1772 (1971).
[19] D. Vanmaekelbergh and F. Cardon, J. Phys. D **19**, 643 (1986).
[20] D. Vanmaekelbergh, W. P. Gomes, and F. Cardon, J. Electrochem. Soc. **134**, 891 (1987).
[21] G. Oskam and P. C. Searson (unpublished).
[22] D. Vanmaekelbergh, A. R. de Wit, and F. Cardon, J. Appl. Phys. **73**, 5049 (1993).